JOURNAL OF SPACECRAFT AND ROCKETS
Vol. 39, No. 5, September–October 2002

Supersonic/Hypersonic Flutter and Postflutter of Geometrically Imperfect Circular Cylindrical Panels

Liviu Librescu* and Piergiovanni Marzocca†
Virginia Polytechnic Institute and State University, Blacksburg, Virginia 24061-0219
and
Walter A. Silva‡
NASA Langley Research Center, Hampton, Virginia 23681-2199

A theoretical investigation of the flutter and postflutter of infinitely long thin-walled circular cylindrical panels in a supersonic/hypersonic flowfield is presented. In this context, third-order piston theory and shock wave aerodynamics are used in conjunction with the geometrically nonlinear shell theory to obtain the pertinent aeroelastic governing equations. The effects of in-plane edge restraints and small initial geometric imperfections are also considered in the model. The objective is twofold: 1) to analyze the implications of nonlinear unsteady aerodynamics and structural nonlinearities on the character of the flutter instability boundary and 2) to outline the effects played, in the same respect, by a number of important geometrical, physical, and aerodynamic parameters characterizing the aeroelastic system. As a by-product of this analysis, the implications of these parameters on the linearized flutter instability behavior of the system are captured and emphasized. The behavior of the aeroelastic system in the vicinity of the flutter boundary is studied via the use of an encompassing methodology based on the Lyapunov first quantity. Numerical illustrations, supplying pertinent information on the implications of geometric and aerodynamic nonlinearities, as well as of other effects, such as curvature and thickness ratios, on the flutter instability and on the character of the flutter boundary are examined, and pertinent conclusions are outlined.

Nomenclature

a_∞	=	speed of sound of undisturbed flow, m/s
b	=	panel width, m
D	=	flexural panel stiffness $[\equiv Eh^3/12(1-\mu^2)]$, N · m
E	=	elastic modulus, Pa
$H, \hat{H}$	=	rise of cylindrical panel, m; its dimensionless counterpart $[\equiv H/R = 1 - \cos(0.5\hat{h}/\bar{h})]$, respectively
$h, \bar{h}$	=	panel thickness, m; its dimensionless counterpart $(\equiv h/b)$, respectively
$\hat{h}$	=	curvature ratio $(\equiv h/R)$
K_x, K_y; R_x, R_y	=	streamwise and spanwise curvatures, 1/m; respective radii of curvature in x, y directions, m
L	=	Lyapunov first quantity
M_F, V_F	=	Mach flutter and flutter speed, respectively, m/s
M_∞, q_∞	=	undisturbed flight Mach number and dynamic pressure $(\equiv \rho_\infty U_\infty^2/2)$, respectively, kg/m s^2
m, n, c	=	roots of the characteristic equation, Eqs. (39)
N_x, N_y, N_{xy}	=	in-plane stress resultants, measured per unit length of the panel cross section, N/m
p, q, r, s	=	coefficients of the characteristic equation, Eqs. (35)
p_∞	=	freestream pressure of the undisturbed flow, Pa
$q_a, \bar{p}$	=	pressure difference $p - p_\infty$, Pa; its dimensionless counterpart $(\equiv q_a/\rho_\infty U_\infty^2)$, respectively
$q_n, \mathring{q}_n$	=	generalized coordinate and amplitude of geometric imperfection, respectively; $n = 1, 2, \ldots$
R	=	radius of curvature
$\Re$	=	boundary of the region of stability
$t, \bar{t}$	=	time, s; its dimensionless counterpart $(\equiv t\Omega)$, respectively
U_∞	=	air speed of undisturbed flow, m/s
u, v, w; $\bar{w}, \mathring{\bar{q}}$	=	displacements in the x, y, z, directions, m; dimensionless transverse deflection $(\equiv w/b)$ and geometric imperfection $(\equiv \mathring{w}/b)$, respectively
v_z	=	downwash velocity normal to the cylindrical panel, m/s
$x, y; z; \bar{y}$	=	in-plane, m; out of plane, m; dimensionless coordinate $(\equiv y/b)$, respectively
γ	=	Glauert's aerodynamic correction factor
Δ_y	=	end-shortening in the y direction
δ_{ij}	=	tracers identifying the linear and nonlinear aerodynamic terms, $i = 1, 2, 3$; $j = y, t$
$\mathring{\delta}_S$	=	tracer identifying the geometrical imperfection
$\varepsilon_x, \varepsilon_y, \varepsilon_{xy}$	=	in-plane strain
κ	=	isentropic gas coefficient
λ_F	=	normalized flutter dynamic pressure $(\equiv 2q_\infty b^3/D)$
μ	=	Poisson's ratio
ξ	=	parameter identifying the movability or immovability of panel edges $y = 0, b$
$\rho_p, \bar{\rho}$	=	panel mass density, kg/m^3; its dimensionless counterpart $(\equiv \rho_p/\rho_\infty)$, respectively
ρ_∞	=	air density of undisturbed flow, km/m^3
$\sigma_x, \sigma_y, \sigma_{xy}$	=	in-plane stress components, N/m^2
ϕ	=	Airy's function
$\Omega, \bar{\Omega}$	=	first natural frequency of a plate panel, rad/s, and its dimensionless counterpart $(\equiv \Omega b/a_\infty)$, respectively
ω	=	frequency, rad/s
$\bar{\omega}_n$	=	ω_n/Ω

Subscripts

$,t; ,tt$	=	$\partial(\cdot)/\partial t; \partial^2(\cdot)/\partial t^2$

Received 10 August 2001; revision received 14 May 2002; accepted for publication 26 June 2002.

*Professor of Aeronautical and Mechanical Engineering, Department of Engineering Science and Mechanics; librescu@vt.edu.
†Visiting Assistant Professor, Engineering Science and Mechanics Department; piermz@vt.edu. Member AIAA.
‡Senior Research Scientist, Senior Aerospace Engineer, Aeroelasticity Branch, Structures and Materials Competency; w.a.silva@larc.nasa.gov. Senior Member AIAA.

$,y;\ ,xy$ = $\partial(\cdot)/\partial y;\ \partial^2(\cdot)/\partial x\partial y$
$+, -$ = quantity evaluated on the upper ($z > 0$) and lower surfaces of the panel, ($z < 0$)

Superscripts

$\bar{}$ = dimensionless quantities
$\mathring{}$ = initial geometric imperfection

Introduction

PANEL flutter is an aeroelastic instability experienced by the skin panels of high-speed flight vehicles in which the structure is exposed to high supersonic flow on one side and to still air on the other side. As a result of structural nonlinearities, which are inherently present, flutter amplitudes remain bounded in a limit-cycle motion.[1] In such conditions, due to high oscillation frequencies, fatigue failure of the panel may occur. On the other hand, due to aerodynamic nonlinearities, a behavior opposite in character can emerge, in the sense that at high flight Mach numbers the flutter boundary can become a catastrophic one. Because the various nonlinearities, for example, structural and aerodynamic, can influence differently the character of the flutter boundary,[2–5] the need to approach the flutter instability by including these effects becomes obvious. The lifting surface or the panels of the rocket body can include concentrated (free-play, damping, hysteresis, preload)[6,7] or distributed nonlinearities that, in addition to the aerodynamic nonlinearities, determine the nature of the flutter boundary. A review of various types of structural nonlinearities and their associated aeroelastic effects has been given by Breitbach.[6]

In spite of the considerable scientific and practical importance in the design of panels of high-speed flight vehicles, such as aircraft, rockets, and launch/reusable vehicles, little work on nonlinear aeroelasticity and flutter of curved structures has been accomplished so far[4,8–12]; the main bulk of the literature has been restricted to the flutter of flat panels.[13–19]

For pertinent and complementary studies on various topics related to the panel flutter, the reader is referred to books by Librescu[4] and Dowell.[1] In recent years, there has been renewed interest in supersonic and hypersonic flight vehicles, and a review of the nonlinear panel flutter has been accomplished by Mei et al.,[14] whereas a review of the finite element method within a linearized approach of the supersonic panel flutter was given by Bismarck-Nasr.[15] In Refs. 17 and 18, both structural and aerodynamic nonlinearities associated with the transonic flow have been included.

One essential limitation of the linearized analysis of the problem is that it gives information only up to the point of instability. Furthermore, the linearized analysis is restricted to cases where the aeroelastic response is small. Often this assumption is violated before the onset of instability. Thus, to study the behavior of aeroelastic systems near the boundary of instability or in the postinstability region, the inherent nonlinearities of structural and aerodynamic nature must be accounted for.

For a better understanding of the implications of important factors rendering the flutter instability boundary benign or catastrophic, the structural and aerodynamic nonlinearities as well as the panel curvature will be included.[2,4] In contrast to the case of the benign flutter boundary, the evolution of the aeroelastic system in the vicinity of the flutter boundary for the case of the catastrophic flutter boundary, even before its occurrence, can result in its catastrophic failure.[1,2] These considerations are intended to emphasize that the nonlinear approach of aeronautical/aerospace structural systems permits determination of the conditions under which undamped oscillations can occur at velocities below the flutter speed (in this case the flutter boundary is catastrophic) and also the conditions under which the flight speed can be exceeded beyond the flutter instability, without catastrophic failure (in this case the flutter boundary is benign). From the mathematical point of view, the issue of the character of the flutter boundary, that is, benign or catastrophic, can be revealed via determination of the nature of the Hopf[20] bifurcation that is, supercritical or subcritical, respectively, as featured by the nonlinear aeroelastic system.

The concept of catastrophic and benign types of flutter are found in the specialized literature under different connotations. The terminology of benign or catastrophic flutter[2,4,5] is synonymous with that of stable and unstable limit-cycle oscillation (LCO),[1,19,21] also referred to as supercritical and subcritical Hopf bifurcation[20] (also Ref. 22), respectively. These terminologies are used throughout the paper.

Aeroelastic Governing Equations

The goals of this paper are, among others, to advance the understanding of the implications of a number of effects that contribute to the occurrence of the catastrophic aeroelastic failure of structural panels. A better understanding of this issue will contribute to a safer design with evident beneficial implications. In the present paper, the geometrically nonlinear theory of infinitely long circular cylindrical open panels is used to derive the aeroelastic governing equations.

In this context, the Kirchhoff–Love shell model in conjunction with von Kármán nonlinear-type approximation is adopted, and in addition, the effect of the free-stress geometric imperfection is included. In the general case of doubly curved shells, the pertinent equations expressed in terms of the transverse deflection w and the Airy function ϕ are

$$(D/h)\nabla^4 w = (w_{,xx} + K_x)\phi_{,yy} + (w_{,yy} + K_y)\phi_{,xx} - 2w_{,xy}\phi_{,xy} + q_a/h - \rho_p w_{,tt} \tag{1}$$

where $D \equiv h^3 E/12(1-\mu^2)$, E is Young's modulus, and q_a is the transversal pressure difference. Equation (1) is referred to as the bending equation of motion. The second equation is obtained by using the compatibility equation:

$$(1/E)\nabla^4\phi = w_{,xy}^2 - w_{,xx}w_{,yy} - K_y\phi_{,xx} - K_x\phi_{,yy} \tag{2}$$

For infinitely long curved panels, the variation of all field quantities in the x direction fulfils the condition $(\cdot)_{,x} = 0$, and, in addition,

$$u = 0, \qquad v = v(y,t), \qquad w = w(y,t) \tag{3}$$

(Fig. 1). In the present study, a circular cylindrical panel will be considered, which implies

$$K_x \equiv 1/R_x = 0, \qquad K_y \equiv 1/R_y = 1/R \tag{4}$$

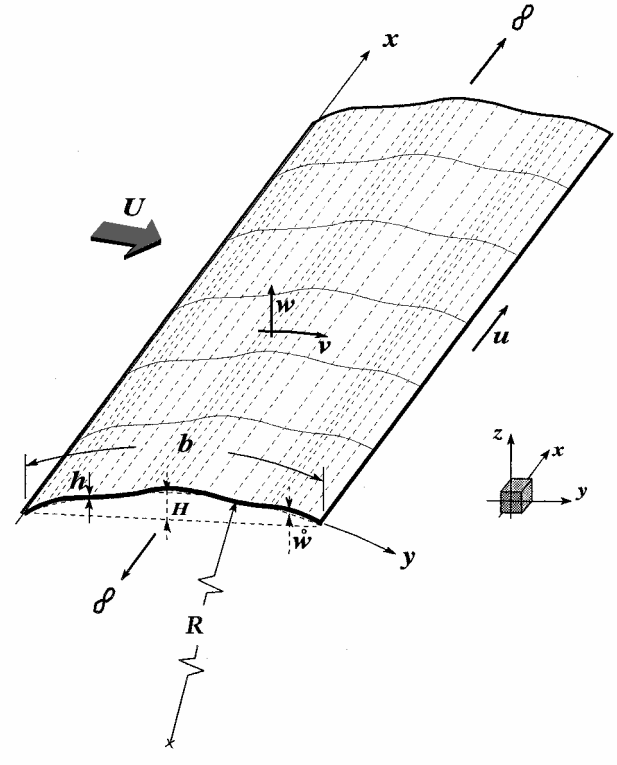

Fig. 1 Circular cylindrical panel geometry.

R is the constant radius of curvature of the reference surface. Notice that, under these conditions, the second von Kármán equation (2) becomes immaterial.

It has been assumed that $\sigma_y \to \sigma$, that is, the tangential stresses act only in the y direction. Physically, this stress is generated by the constraint of the panel with the members of the airframe. As a result, for the in-plane stress resultants, N_x, N_y, and N_{xy}, we have

$$\sigma_x = N_x/h = \phi_{,yy} = E/(1-\mu^2)(\varepsilon_x + \mu\varepsilon_y) = 0 \tag{5}$$

$$\sigma_y = N_y/h = \phi_{,xx} = E/(1-\mu^2)(\varepsilon_y + \mu\varepsilon_x) \equiv \sigma \tag{6}$$

$$\sigma_{xy} = N_{xy}/h = -\phi_{,xy} = E/(1+\mu)\varepsilon_{xy} = 0 \tag{7}$$

where ϕ is Airy's potential function. In the light of the earlier stated assumptions, Eq. (1) becomes

$$(D/h)w_{,yyyy} = (w_{,yy} + 1/R)\sigma_y + q_a/h - \rho_p w_{,tt} \tag{8}$$

To evaluate the tangential stress component σ_y, one expresses the average end shortening, enabling one to evaluate the in-plane load σ_y in the form

$$\Delta_y(t) = \frac{1}{b}\int_0^b \frac{\partial v(y,t)}{\partial y}\,\mathrm{d}y \tag{9}$$

On the other hand, based on the expressions of the strain–displacement relationship expressed in Lagrangian description, adoption of von Kármán assumption, and inclusion of the initial geometric imperfection $\mathring{w}$, the strain in the y direction, ε_y, becomes

$$\varepsilon_y = v_{,y} + \tfrac{1}{2}(w_{,y})^2 + w_{,y}\mathring{w}_{,y} - w/R \qquad (y \rightleftarrows x) \tag{10}$$

When the expression of ε_y obtained from

$$\sigma_y = E/(1-\mu^2)(\varepsilon_y + \mu\varepsilon_x) \tag{11}$$

is used in Eq. (10) in conjunction with that $\varepsilon_x = 0$, one obtains

$$\sigma_y = E/(1-\mu^2)\left[v_{,y} + \tfrac{1}{2}(w_{,y})^2 - w/R + w_{,y}\mathring{w}_{,y}\right] \tag{12}$$

Solving now Eq. (12) for $v_{,y}$, one obtains

$$v_{,y} = (\sigma_y/E)(1-\mu^2) - \tfrac{1}{2}(w_{,y})^2 + w/R - w_{,y}\mathring{w}_{,y} \tag{13}$$

Applying the operator

$$\frac{1}{b}\int_0^b (\cdot)\,\mathrm{d}y$$

to Eq. (13), in conjunction with Eq. (9), one obtains the end shortening in the y direction. For $\Delta_y = 0$, that is, when the edges $y = 0, b$ are immovable,

$$\int_0^b v_{,y}\,\mathrm{d}y = 0 \Longrightarrow \Delta_y = 0 \tag{14}$$

Equation (14), in conjunction with Eq. (13), yields

$$\sigma_y = \frac{E}{b(1-\mu^2)}\left[\frac{1}{2}\int_0^b (w_{,y})^2\,\mathrm{d}y - \int_0^b \frac{w}{R}\,\mathrm{d}y + \int_0^b w_{,y}\mathring{w}_{,y}\,\mathrm{d}y\right] \tag{15}$$

Substitution of Eq. (15) in Eq. (8) results in

$$Dw_{,yyyy} - \frac{Eh}{b(1-\mu^2)}\left[\frac{1}{2}\int_0^b (w_{,y})^2\,\mathrm{d}y - \int_0^b \frac{w}{R}\,\mathrm{d}y + \int_0^b w_{,y}\mathring{w}_{,y}\,\mathrm{d}y\right]\left(w_{,yy} + \frac{1}{R}\right) - q_a + \rho_p h w_{,tt} = 0 \tag{16}$$

Equation (16) represents the geometrically nonlinear governing equation of infinitely long circular cylindrical panels with immovable edges, incorporating the initial geometric imperfections. Notice that, for flat geometrically perfect panels, that is, when $R \to \infty$ and $\mathring{w} = 0$, Eq. (16) reduces to a form extensively used in nonlinear panel flutter investigations (for example, see Refs. 1 and 14), namely,

$$Dw_{,yyyy} - \frac{Eh}{2b(1-\mu^2)}w_{,yy}\int_0^b (w_{,y})^2\,\mathrm{d}y - q_a + \rho_p h w_{,tt} = 0 \tag{17}$$

Piston Aerodynamic Theory and Shock Wave Aerodynamics

In this paper, both third-order piston theory and shock wave aerodynamics are used to address the nonlinear panel flutter. Piston theory aerodynamics, advanced by Lighthill[23] in problems of oscillating airfoils and later used[24] as an aeroelastic tool, is a popular modeling technique for supersonic and hypersonic aeroelastic analyses. Consistent with piston theory aerodynamics (PTA), the unsteady pressure can be expressed as

$$p(y,t) = p_\infty\{1 + [(\kappa-1)/2](v_z/a_\infty)\}^{2\kappa/(\kappa-1)} \tag{18}$$

where the downwash velocity v_z normal to the cylindrical panel and the undisturbed speed of sound a_∞ are expressed as

$$v_z = -(w_{,t} + U_\infty w_{,y}), \qquad a_\infty^2 = \kappa p_\infty/\rho_\infty \tag{19}$$

where $\kappa = 1.4$ for dry air. In the binomial expansions of Eq. (18), retaining the terms up to and including $(v_z/a_\infty)^3$ yields the pressure formula for the PTA in the third-order approximation[2,4,25–27]:

$$p/p_\infty = 1 + \kappa(v_z/a_\infty)\gamma + [\kappa(\kappa+1)/4][(v_z/a_\infty)\gamma]^2 + [\kappa(\kappa+1)/12][(v_z/a_\infty)\gamma]^3 \tag{20}$$

The linear term of this expression corresponds to Ackeret's formula for the quasi-steady pressure on a thin profile in a supersonic flowfield, whereas the quadratic term is from Busemann's formula for $M_\infty^2 \gg 1$ (see Ref. 4). In Eq. (20), the aerodynamic correction factor, $\gamma = M_\infty/\sqrt{(M_\infty^2 - 1)}$, enables one to extend the validity of the PTA to the entire low supersonic–hypersonic flight speed regime. Also note that Eqs. (18–20) are applicable as long as the transformations through compression and expansion may be considered as isentropic, that is, as long as the induced shock losses would be negligible (low intensity waves). However, Eq. (20) does not take into account the losses across a shock, nor does it accurately predict the pressure in an area associated with heavy shock interactions.[27] For more details, see Refs. 28 and 29. A more general formula for the pressure, obtained from the theory of oblique shock waves (SWT) that is valid over the entire supersonic–hypersonic flight speed range and valid both for compression before the shock wave and for expansion (assuming that the shock waves are attached to the sharp leading edge and that the flow behind these waves remains supersonic) is given by[29]

$$p/p_\infty = 1 + \kappa(v_z/a_\infty)\gamma + [\kappa(\kappa+1)4][(v_z/a_\infty)\gamma]^2 + [\kappa(\kappa+1)^2/32][(v_z/a_\infty)\gamma]^3 \tag{21}$$

Equations (20) and (21) are identical, with the exception of the cubic terms appearing therein. This is because the entropy variation appears in the pressure expansion, beginning with the third-order terms. Moreover, Eq. (21) encompasses a number of advantages such as the following: 1) It takes into account for the shock losses occurring in the case of strong waves, 2) It can be used over a larger range of angles of attack ($\alpha \leq 30$ deg) and Mach numbers ($M_\infty \geq 1.3$), and 3) It is also valid for the Newtonian speed regime ($M_\infty \to \infty$; $\kappa \to 1$) (Ref. 29).

Comparisons of results related to the catastrophic and benign character of the flutter boundary as derived from these two formulations of unsteady aerodynamic loads are presented herein. The two cubic term coefficients differ by 10% for $\kappa = 1.4$, which is estimated by comparing $(5-3\kappa)/8$ with unity; thus, for a better prediction of the character of the flutter instability boundary, it has to be included.[23] This difference increases with the increase of the Mach number. However, within the linear stability analysis, it is evident, as it should be, that the flutter speed evaluated with these two expressions coincide.

Moreover, the SWT, which considers the pressure losses through shock waves, provides more accurate predictions compared to PTA. However, in a number of cases, the contribution of these terms to the total pressure turns out to be marginal. In such a case, the use of Eq. (20), instead of the more exact Eq. (21), constitutes a preferable option. As reported in Ref. 30, PTA provides results in excellent agreement with those based on the Euler solution and the CFL3D code. In the low supersonic flight speed regime, the PTA and SWT corrected by γ provide a rather good agreement with the supersonic flow theory,[31] and so this correction should be included.

The start of the hypersonic flight speed regime is not clear cut. Generally, speeds above Mach 5 are considered hypersonic. This is the speed at which the aerodynamic heating becomes important in aircraft design. Because this effect will not affect the conclusions about the implications of the considered nonlinearities, the effects of the nonuniform temperature field are not included here. For the panel flutter problem in the presence of thermal loads, the interested reader is referred to Refs. 5, 32, and 33.

In the following developments, unless otherwise stated, piston theory aerodynamics has been applied. When the flow is considered to take place only on the upper surface of the panel $U_\infty^+ \equiv U_\infty$ and $M_\infty = U_\infty^+/a_\infty$, that is, when $U_\infty^- = 0$ and $p^- = p_\infty$ are considered, from Eqs. (18–20), the aerodynamic pressure difference can be expressed as

$$q_a = p - p_\infty = \delta p\,|_{\mathrm{PTA}} = -(2q_\infty/M_\infty)\gamma\left\{(1/U_\infty)w_{,t} + w_{,y} + [(1+\kappa)/4]\gamma M_\infty \times [(1/U_\infty)w_{,t} + w_{,y}]^2 + [(1+\kappa)/12]\gamma^2 M_\infty^2[(1/U_\infty)w_{,t} + w_{,y}]^3\right\} \tag{22}$$

where the undisturbed flight Mach number $M_\infty = U_\infty/a_\infty$ and the undisturbed dynamic pressure $q_\infty = \rho_\infty U_\infty^2/2$. When the flow takes place on both surfaces of the panel (with the speed $U_\infty^+ = U_\infty^- = U_\infty$), the quadratic term vanishes, and so only the linear and nonlinear cubic terms subsist. Although, this is an important case that involves the aeroelasticity of lifting surfaces, here only the case of panel flutter has been addressed. As a result, the expression of the aerodynamic pressure difference in Eq. (22) has been accordingly modified.

When the dimensionless parameters $\bar{h} = h/b$, $\hat{h} = h/R$, and $\bar{\Omega} = \Omega b/a_\infty$ are considered, where Ω is the first natural frequency of the flat panel counterpart, Eq. (16) reduces to $W[\bar{w}(\bar{y}, \bar{t})] = 0$, where

$$W(\bar{w}(\bar{y},\bar{t})) \equiv \bar{w}_{,\overline{yyyy}} - \frac{12}{\bar{h}^2}\xi\left[\frac{1}{2}\int_0^1 (\bar{w}_{,\bar{y}})^2\,\mathrm{d}\bar{y} - \frac{\hat{h}}{\bar{h}}\int_0^1 \bar{w}\,\mathrm{d}\bar{y} + \overset{\bullet}{\delta}_s\int_0^1 \bar{w}_{,\bar{y}}\overset{\bullet}{\bar{w}}_{,\bar{y}}\,\mathrm{d}\bar{y}\right]\left(\bar{w}_{,\overline{yy}} + \frac{\hat{h}}{\bar{h}}\right) + \frac{M_\infty \pi^4}{\bar{\rho}\bar{h}\bar{\Omega}^2}\gamma \times \left[\delta_{1t}\frac{\bar{\Omega}}{M_\infty}\bar{w}_{,\bar{t}} + \delta_{1y}\bar{w}_{,\bar{y}} + \frac{1+\kappa}{4}\gamma M_\infty\left(\delta_{2t}\frac{\bar{\Omega}}{M_\infty}\bar{w}_{,\bar{t}} + \delta_{2y}\bar{w}_{,\bar{y}}\right)^2 + \frac{1+\kappa}{12}\gamma^2 M_\infty^2\left(\delta_{3t}\frac{\bar{\Omega}}{M_\infty}\bar{w}_{,\bar{t}} + \delta_{3y}\bar{w}_{,\bar{y}}\right)^3\right] + \pi^4\bar{w}_{,\overline{tt}} = 0 \tag{23}$$

In Eq. (23) various tracers δ_{ij} and $\overset{\bullet}{\delta}_s$ have been included to identify various effects. The first index of the tracer δ_{ij}, $i = 1, 2, 3$, identifies the linear ($i = 1$), quadratic ($i = 2$), and cubic ($i = 3$) nonlinear aerodynamic terms, whereas the second index $j = y, t$, identifies the derivatives of $\bar{w}$ with respect to $\bar{y}$ or $\bar{t}$. The latter terms represent the contributions of the aerodynamic damping. In addition, tracer $\overset{\bullet}{\delta}_s$ identifies the geometrical imperfection. When these terms are discarded, $\delta_{ij} = \overset{\bullet}{\delta}_s = 0$, otherwise $\delta_{ij} = \overset{\bullet}{\delta}_s = 1$. Also in Eq. (23) the conditions of movability or immovability of the cylindrical panel edges have been identified via incorporation of the parameter ξ, where $\xi = 1$ implies immovable edges and $0 \le \xi < 1$ implies that the edges feature various degrees of movability.

Natural Frequencies

In the case of geometrically linear perfect panel and in the absence of aerodynamic loads, Eq. (23) reduces to

$$\bar{w}_{,\overline{yyyy}} + \frac{12}{\bar{h}^2}\left(\frac{\hat{h}}{\bar{h}}\right)^2\int_0^1 \bar{w}\,\mathrm{d}\bar{y} + \pi^4\bar{w}_{,\overline{tt}} = 0 \tag{24}$$

For cylindrical panels simply supported on $\bar{y} = (0, 1)$, expressing $\bar{w}(\bar{y}, \bar{t})$ in the form $\bar{w}(\bar{y}, \bar{t}) = w_1 \sin(\pi\bar{y})\sin(\bar{\omega}_1\bar{t})$, the first natural frequency is obtained as

$$\bar{\omega}_1^2 = \omega_1^2/\Omega^2 = 1 + (96/\pi^6\bar{h}^2)(\hat{h}/\bar{h})^2 \tag{25}$$

For the flat panel its counterpart is $\bar{\omega}_1^2 = 1$. The natural eigenfrequencies of the simply supported cylindrical panel can be expressed in a general form as

$$\bar{\omega}_m^2 = m^4 + \frac{24}{\pi^4\bar{h}^2}\left(\frac{\hat{h}}{\bar{h}}\right)^2\left[\frac{1-\cos(m\pi)}{m\pi}\right]^2, \qquad m = 1, 2, 3, \ldots \tag{26}$$

From Eq. (25) it clearly appears that, although the even mode natural frequencies for a circular shell coincide with those of flat panels, the odd mode natural frequencies are higher than their flat panel counterparts.

Solution Methodology

For the solution of the nonlinear flutter problem, Fung[34] used the harmonic balance technique; Bolotin,[5] Eastep and McIntosh,[35] Dowell,[9–12] Bolotin et al.,[16] and Amabili and Pellicano[8] employed the direct numerical integration technique, whereas Morino[36] used perturbation methods. More recently, limit-cycle amplitude panel flutter (LCO) using the finite element method was studied.[14,15,37,38] In the present approach, an analytical formulation based on the Lyapunov first quantity[2–4] in conjunction with Galerkin's method enables one to evaluate the character of the flutter boundary.

As a reminder, Eq. (23) has to be solved in conjunction with given boundary conditions. For the case of simply supported panels on $\bar{y} = 0, 1$, it is required that $\bar{w} = \bar{w}_{,\overline{yy}} = 0$. Galerkin's method is used by expressing $\bar{w}(\bar{y}, \bar{t})$ and $\overset{\bullet}{\bar{w}}(\bar{y})$ in the form

$$\{\bar{w}(\bar{y},\bar{t}),\ \overset{\bullet}{\bar{w}}(\bar{y})\} = \sum_{n=1}^{\infty}\{q_n(\bar{t}),\ \overset{\bullet}{q}_n\}f_n(\bar{y}) \tag{27}$$

When modal functions $f_n(\bar{y}) = \sin(\lambda_n\bar{y})$ and $\lambda_n = n\pi$, $n = 1, 2, \ldots$, are considered, all of the boundary conditions that concern the transverse deflection $\bar{w}$ are fulfilled. The generalized coordinates $q_n(\bar{t})$ are time-dependent functions. Replacement of Eq. (27) into Eq. (23) yields a residual term that should be minimized in the Galerkin's sense:

$$\int_0^1 W(\bar{y},\bar{t})f_m(\bar{y})\,\mathrm{d}\bar{y} = 0 \tag{28}$$

Under an explicit form, the residual function $W(\bar{y}, \bar{t})$ is written as

$$W(\bar{y},\bar{t}) \equiv \sum_{n=1}^{k}\lambda_n^4 q_n(\bar{t})\sin(\lambda_n\bar{y}) + \pi^4\sum_{n=1}^{\infty} q_n(\bar{t})_{,\overline{tt}}\sin(\lambda_n\bar{y}) + \frac{12}{\bar{h}^2}\xi\left\{\frac{1}{2}\int_0^1\left[\sum_{n=1}^{\infty}\lambda_n q_n(\bar{t})\cos(\lambda_n\bar{y})\right]^2\mathrm{d}\bar{y} - \frac{\hat{h}}{\bar{h}}\int_0^1\sum_{n=1}^{\infty} q_n(\bar{t})\sin(\lambda_n\bar{y})\,\mathrm{d}\bar{y} + \overset{\bullet}{\delta}_s\int_0^1\sum_{n=1}^{\infty}\lambda_n q_n(\bar{t})\cos(\lambda_n\bar{y}) \times \sum_{n=1}^{\infty}\lambda_n\overset{\bullet}{q}_n\cos(\lambda_n\bar{y})\,\mathrm{d}\bar{y}\right\}\left[\sum_{n=1}^{\infty}\lambda_n^2 q_n(\bar{t})\sin(\lambda_n\bar{y}) - \frac{\hat{h}}{\bar{h}}\right]$$

$$+\frac{M_\infty \pi^4}{\bar{\rho}\bar{h}\bar{\Omega}^2}\gamma\left\{\delta_{1t}\frac{\bar{\Omega}}{M_\infty}\sum_{n=1}^{\infty}q_n(\bar{t})_{,\bar{t}}\sin(\lambda_n\bar{y})\right.$$

$$+\delta_{1y}\sum_{n=1}^{\infty}\lambda_n q_n(\bar{t})\cos(\lambda_n\bar{y})+\sum_{n=1}^{\infty}\lambda_n\dot{q}_n\cos(\lambda_n\bar{y})+\frac{1+\kappa}{4}\gamma M_\infty$$

$$\times\left[\delta_{2t}\frac{\bar{\Omega}}{M_\infty}\sum_{n=1}^{\infty}q_n(\bar{t})_{,\bar{t}}\sin(\lambda_n\bar{y})+\delta_{2y}\sum_{n=1}^{\infty}\lambda_n q_n(\bar{t})\cos(\lambda_n\bar{y})\right]^2$$

$$+\frac{1+\kappa}{12}\gamma^2M_\infty^2\left[\delta_{3t}\frac{\bar{\Omega}}{M_\infty}\sum_{n=1}^{\infty}q_n(\bar{t})_{,\bar{t}}\sin(\lambda_n\bar{y})\right.$$

$$\left.\left.+\delta_{3y}\sum_{n=1}^{\infty}\lambda_n q_n(\bar{t})\cos(\lambda_n\bar{y})\right]^3\right\}=0 \tag{29}$$

As a result of Eq. (28), a set of nonlinear, simultaneous differential equations with respect to the coefficients of the series in Eq. (27) is obtained. In condensed form it is written as

$$\frac{\mathrm{d}^2q_m}{\mathrm{d}\bar{t}^2}+g\frac{\mathrm{d}q_m}{\mathrm{d}\bar{t}}+F_m(q_n,M_\infty)=0,\qquad n,m=1,2,3,\ldots \tag{30}$$

The term $g\,\mathrm{d}q_m/\mathrm{d}\bar{t}$ associated with the structural damping has been discarded. Although structural damping can be included in the analysis, the present simulations involve only aerodynamic damping. In such a context, more conservative estimates of the flutter speed are expected to occur. The functions $F_m(q_{nm}, M_\infty)$ can be represented as

$$F_m(q_n,M_\infty)=F_m^{(l)}(q_n,M_\infty)+F_m^{(a)}(q_n,M_\infty)+F_m^{(s)}(q_n,M_\infty) \tag{31}$$

where $F_m^{(l)}(q_n, M_\infty)$ are linear functions and $F_m^{(a)}(q_n, M_\infty)$ and $F_{nm}^{(s)}(q_n, M_\infty)$ are functions including the aerodynamic and structural nonlinearities, respectively. Note that, within the structural nonlinearities, the curvature is connected with the quadratic terms.[2] To solve the linearized problem resulting in the evaluation of the flutter characteristics, $q_n(\bar{t})$ can be expressed as

$$q_n(\bar{t})=\sum_{n=1}^{k}a_n e^{i\bar{\omega}_n\bar{t}} \tag{32}$$

where i is the imaginary unit.

Stability in the Vicinity of the Critical Flutter Boundary

As already stated, the conditions of catastrophic/benign character of the flutter instability boundary are obtained via the use of the Lyapunov first quantity L (Refs. 2–4 and 39). For the problem at hand, this quantity will be evaluated next.

To this end, the system of governing equations (30) is converted to a system of four differential equations in state-space form expressed generically as[4,40]

$$\frac{\mathrm{d}x_j}{\mathrm{d}t}=\sum_{m=1}^{n}a_m^{(j)}x_m+P_j(x_1,x_2,\ldots,x_n),\qquad j=\overline{1,4} \tag{33}$$

As will be seen, the matrix $a_m^{(j)}$ in the Appendix contains the aerodynamic submatrix that, in absence of geometrical imperfections, is antisymmetric. For the present case, the functions $P_j(x_1, x_2, \ldots, x_n)$ include both the structural and aerodynamic nonlinear terms that can be cast generically as

$$P_j(x_1,x_2,\ldots,x_n)=\sum_{i=1}^{n}a_{ii}^{(j)}x_i^2+2\sum_{\substack{i,l=1\\(i\neq l)}}^{n}a_{li}^{(j)}x_ix_l+\sum_{i=1}^{n}a_{iii}^{(j)}x_i^3$$

$$+3\sum_{\substack{i,l=1\\(i\neq l)}}^{n}a_{iil}^{(j)}x_i^2x_l+6\sum_{\substack{i,l,k=1\\(i\neq l\neq k)}}^{n}a_{ilk}^{(j)}x_ix_lx_k \tag{34}$$

Equation (33) can be presented in a form that can then be used toward the evaluation of the Lyapunov first quantity $L(M_F)$. To this end, considering the solution of the linearized counterpart of Eq. (33) under the form $x_j = A_j \exp(\omega t)$, one obtains the characteristic equation

$$\omega^4+p\omega^3+q\omega^2+r\omega+s=0 \tag{35}$$

where the quantities p, q, r, and s are supplied in the Appendix.

As a reminder, for steady motion the equilibrium is stable in Lyapunov's sense, if the real parts of all of the roots of the characteristic equation are negative. Such an analysis can be done by using the Routh–Hurwitz's criterion. On this basis, the stability conditions reduce to $p>0$, $q>0$, $r>0$, and $s>0$, and

$$\Re=pqr-sp^2-r^2>0 \tag{36}$$

For the aeroelastic stability problem in which the condition

$$sp/r+p^2/4>0 \tag{37}$$

should be satisfied, the roots of the characteristic equation on the critical flutter boundary $\Re=0$ are given by

$$\omega_{1,2}=\pm ic,\qquad \omega_{3,4}=-m\pm in \tag{38}$$

$$c^2=r/p,\qquad m=p/2,\qquad n^2=sp/r-p^2/4 \tag{39}$$

with $n>0$. For sufficiently small values of the speed, all of the roots of the characteristic equation are in the left half-plane of the complex variable, and the zero solution of the system is asymptotically stable. In addition, when $M_\infty = M_F$ for which the two roots of the characteristic equation are purely imaginary, and the remaining two are complex conjugate and also remain in the left half-plane of the complex variable, the value is critical and corresponds to the critical flutter velocity M_F. These conditions correspond to the one of the Hopf bifurcation theorem.

Then, to identify the benign and catastrophic portions of the stability boundary (or in the terminology of the Hopf bifurcation, the supercritical from the subcritical ones), it is necessary to solve the problem of stability for the system of equations in state-space form in the critical case of a pair of pure imaginary roots. The expression of the boundary of the region of stability $\Re$ for the supersonic panel is defined by

$$\Re=\frac{\gamma^2\delta_{1t}}{\pi^{12}\bar{\rho}^4\bar{\Omega}^4\bar{h}^{10}}\left[9\rho^2\bar{\Omega}^2\left(5\pi^6\bar{h}^4+8\pi^3\xi\dot{q}_1\dot{\delta}_s\bar{h}\hat{h}-32\xi\hat{h}^2\right)^2\right.$$

$$+2\pi^6\gamma^2\delta_{1t}\bar{h}^2\left(17\pi^6\bar{h}^4-24\pi^3\xi\dot{q}_1\dot{\delta}_s\bar{h}\hat{h}+96\xi\hat{h}^2\right)\Big]$$

$$-\frac{1024\dot{q}_2\gamma^3\xi\hat{h}}{\bar{\rho}^3\bar{\Omega}^4\bar{h}^6\pi^3}M_\infty\dot{\delta}_s\delta_{1t}\delta_{1y}-\frac{256\gamma^4}{9\bar{\rho}^4\bar{\Omega}^6\bar{h}^4}M_\infty^2\delta_{1t}\delta_{1y} \tag{40}$$

Notice that this expression is general and includes the relationship between the flutter speed and the flutter frequency parameters evaluated on $\Re=0$ in terms of the basic geometric and aerodynamic parameters. The expression of the flutter instability boundary can be obtained in term of M_F as

$$M_F=\frac{3\bar{\Omega}\delta_{1y}}{16\pi^6\gamma\bar{h}^3}\left[9\rho^2\bar{\Omega}^2\left(5\pi^6\bar{h}^4+8\pi^3\xi\dot{q}_1\dot{\delta}_s\bar{h}\hat{h}-32\xi\hat{h}^2\right)^2\right.$$

$$+2\pi^6\gamma^2\delta_{1t}\bar{h}^2\left(17\pi^6\bar{h}^4-24\pi^3\xi\dot{q}_1\dot{\delta}_s\bar{h}\hat{h}+96\xi\hat{h}^2\right)$$

$$\left.+9216\pi^6\xi^2\bar{\rho}^2\bar{\Omega}^2\dot{q}_2\dot{\delta}_s\bar{h}^2\hat{h}^2\right]^{\frac{1}{2}}-\frac{18\bar{\Omega}^2\bar{\rho}\dot{q}_2\dot{\delta}_s\hat{h}\xi}{\pi^3\gamma\bar{h}^2} \tag{41}$$

As a special case, the expression of the flutter speed evaluated in Ref. 2 for flat plates can be obtained. As also reported in Refs. 41 and 42, from Eq. (41) it clearly appears that the curvature and the imperfections play a significant role on the flutter speed.

Following the method developed by Lyapunov[40] and Bautin,[39] the catastrophic or benign portions of the boundary of the flutter boundary can be determined via the determination of the sign of the Lyapunov first quantity. To this end, the system of Eq. (33) reduced to the canonical form reads

$$\frac{\mathrm{d}\bar{x}_1}{\mathrm{d}\bar{t}} = -c\bar{x}_2 + Q_1(\bar{x}_1, \bar{x}_2, \bar{x}_3, \bar{x}_4)$$

$$\frac{\mathrm{d}\bar{x}_2}{\mathrm{d}\bar{t}} = c\bar{x}_1 + Q_2(\bar{x}_1, \bar{x}_2, \bar{x}_3, \bar{x}_4)$$

$$\frac{\mathrm{d}\bar{x}_3}{\mathrm{d}\bar{t}} = m\bar{x}_3 - n\bar{x}_4 + Q_3(\bar{x}_1, \bar{x}_2, \bar{x}_3, \bar{x}_4)$$

$$\frac{\mathrm{d}\bar{x}_4}{\mathrm{d}\bar{t}} = n\bar{x}_3 - m\bar{x}_4 + Q_4(\bar{x}_1, \bar{x}_2, \bar{x}_3, \bar{x}_4) \qquad (42)$$

where m, n, and c are determined by Eqs. (39). In Eqs. (42), Q_i denotes the nonlinear terms appearing in the canonical counterpart of Eqs. (33). The expression of the Lyapunov first quantity, derived in an analytical way by Bautin,[39] is provided under a closed form in Ref. 4 (Appendix A, pp. 543–552). Following the procedure developed in Refs. 4 and 39, for the present case, the Lyapunov first quantity is expressed in terms of c, m, and n and the coefficients $A_{il}^{(j)}$ and $A_{ilk}^{(j)}$. It is worth noting that the effect of the initial geometric imperfections appears only in linear terms and in $A_{il}^{(j)}$, which represents the quadratic nonlinearities.

The flutter critical boundary is benign, that is, yields stable LCOs, or is catastrophic, that is, yields unstable LCO, if the inequalities

$$L(M_F) < 0, \qquad L(M_F) > 0 \qquad (43)$$

are fulfilled, respectively. As a general comment, the Lyapunov first quantity contains terms related to the structural S and aerodynamic A nonlinearities, and the effect of the curvature C is contained in both the linear term and the structural nonlinearities. As will be shown by the numerical simulations, the combination of these terms significantly affects the character of the flutter boundary. In the region of the benign flutter boundary, the system can slightly exceed the flutter critical speed M_F without catastrophic failure, and as a result, the amplitude of w remains limited. Conversely, in the region of catastrophic flutter boundary, an explosive type of flutter can be experienced.

Results and Discussion

Unless otherwise stated, the numerical simulations consider as a test case an aluminum cylindrical panel whose mechanical properties and geometric parameters are $E = 7 \times 10^{10}$ Pa, $\mu = 0.3$, $\rho_p = 3000$ kg/m^3, $b = 1$ m, $h = 0.01$ m, $R = 10$ m, $\omega_1 = 144.27$ rad/s, $\xi = 1$, and $\dot{q}_1 = \dot{q}_2 = 0$. In addition, for the flowfield characteristics one considers $\rho_\infty = 1.225$ kg/m^3, $\kappa = 1.4$, $\gamma = 1$, and $a_\infty = 340.3$ m/s. As a result, $\bar{h} = 0.01$, $\hat{h} = 0.001$, $\bar{\rho} \approx 2450$, and $\bar{\Omega} = 0.424$. For this test case, the Mach flutter is $M_F = 4.14$, and the dimensionless flutter frequency is $\bar{\omega}_F^2 = 13.5$.

In Figs. 2 and 3, the frequency coalescence vs the flight Mach number are shown. It appears that the flutter speed is obtained from the coalescence of the two consecutive eigenfrequencies.[4] For the infinitely long panels, the axisymmetric modes can be neglected, and the correct nonlinear behavior of the system can still be captured. In the present case, as shown in Fig. 2, the minimum flutter speed is obtained from the coalescence of the first two mode eigenfrequencies, whereas the coalescence of the other successive mode frequencies appears at larger values of the flight speed. As clearly shown in Fig. 3, although a decrease of the flutter speed is obtained for small curvature ratio $\hat{h}(\equiv h/R)$, its increase occurs for large curvature ratios.

Figure 4 reveals the implications of the curvature ratio on the flutter dynamic pressure λ_F. The comparison of the results obtained from the present analysis with consideration of two mode and four mode solutions with those of Refs. 11, 12, and 43 shows very good agreement. Here, the flutter dynamic pressure of the infinitely long cylindrical panel has been normalized with that of the finite length panel of Refs. 11 and 12. As was shown in Refs. 11 and 12, with the

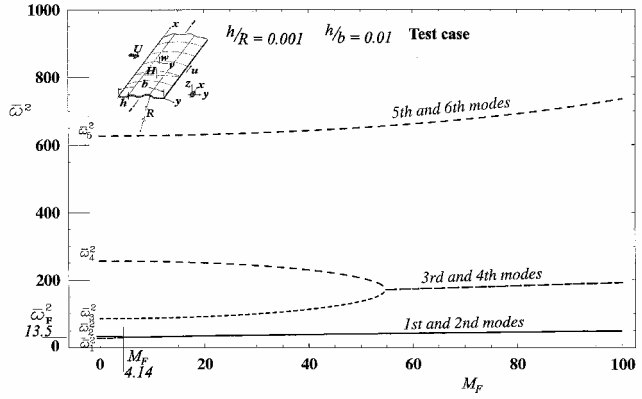

Fig. 2 Frequency coalescence for selected consecutive modes.

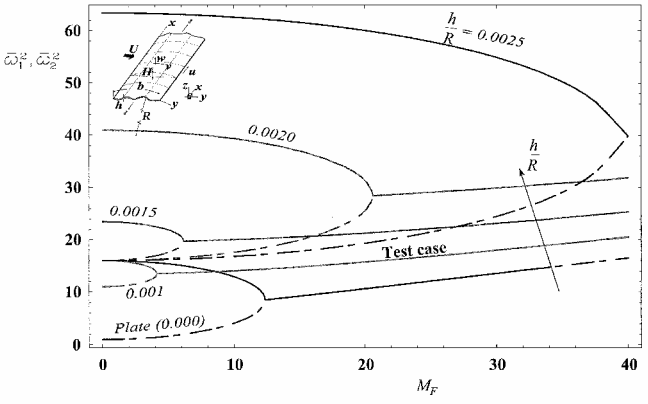

Fig. 3 Frequency coalescence for selected curvature ratio *h/R*.

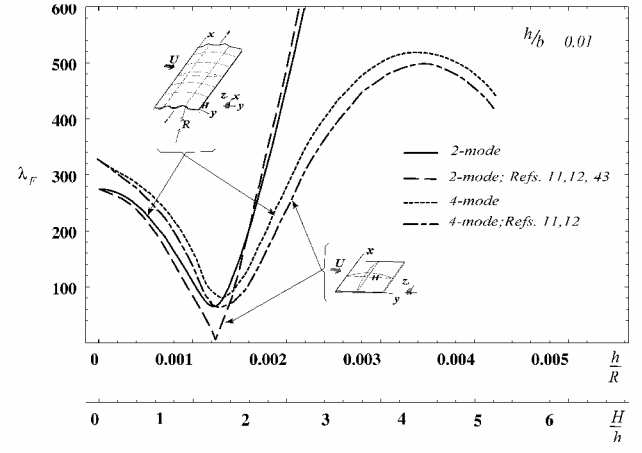

Fig. 4 Comparisons of the flutter dynamic pressure vs the curvature ratio.

linear unsteady aerodynamic and aerodynamic damping taken into account, no local minima of the flutter dynamic pressure are experienced. Because an unrealistic zero value of the dynamic pressure is predicted when the aerodynamic damping is neglected, this effect always has to be included.[11,12,43] With the increase of the curvature ratio, the two-mode solution breaks down, whereas the four-mode solution provides another minimum. As was indicated in Refs. 11 and 12, a solution containing a large number of modes probably would indicate a minimum of the flutter dynamic pressure at all intersections of mode frequencies. However, in a limited range of the curvature ratio, the results emerging from Fig. 4 reveal that there are marginal differences when considering the four-modes solution as compared to the two-modes solution.

As readily seen from Fig. 5, the flutter speed is lower in the case of the flow on both sides of the panel (with $U_\infty^+ = U_\infty^- = U_\infty$) than

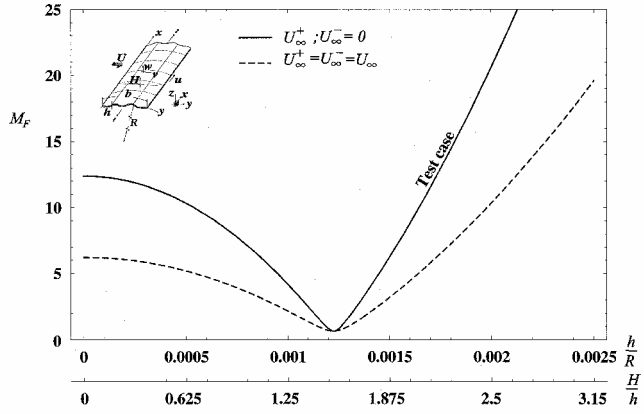

Fig. 5 Flutter speed vs h/R (H/h) for cylindrical panels with flow on one and both sides.

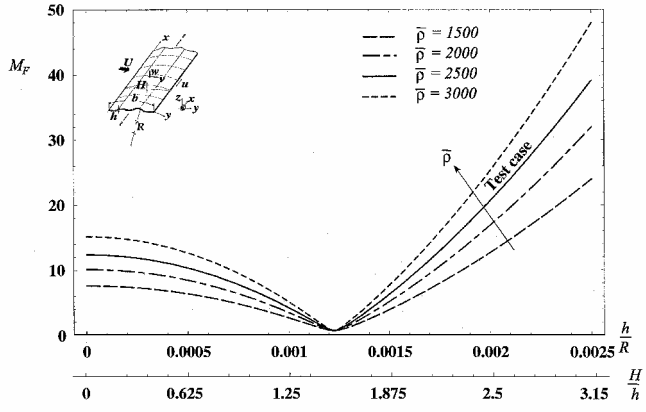

Fig. 6 Flutter speed vs h/R; effect of the mass ratio $\bar{\rho}$.

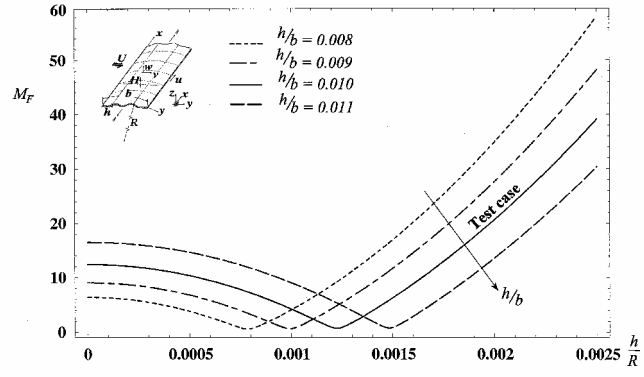

Fig. 7 Effect of the thickness ratio $\bar{h} \equiv h/b$ on the flutter speed vs the curvature ratio.

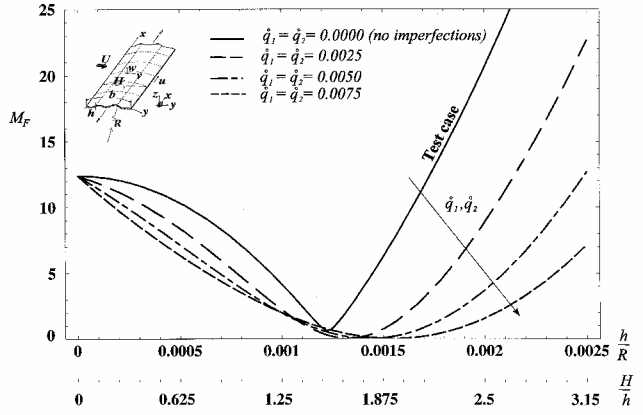

Fig. 8 Effect of the imperfections on the flutter speed vs the curvature ratio.

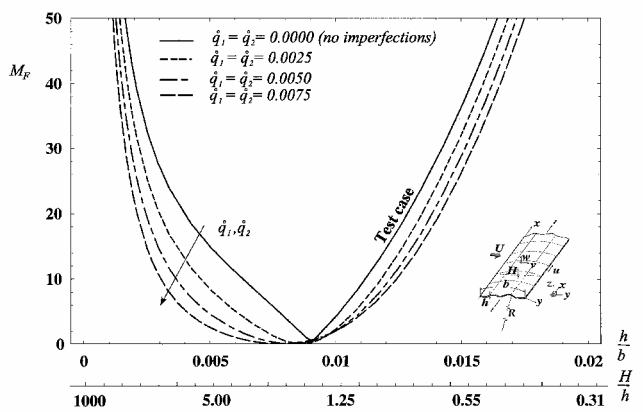

Fig. 9 Effect of the imperfections on the flutter speed vs the thickness ratio.

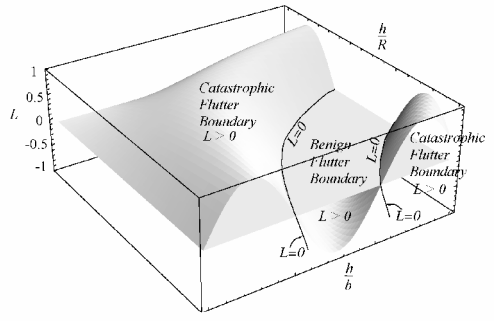

Fig. 10 Generic representation of the catastrophic [$L(M_F) > 0$] and benign flutter [$L(M_F) < 0$], that is, stable LCO portion of the flutter critical boundary.

in the case of the flow on the upper side only ($U_\infty^- = 0$). In this case, the flutter speed of a flat panel is exactly half. With an increase of the curvature ratio, the flutter speed for the case of the flow on one side decreases more rapidly than in the case of the flow on both sides. However, for a particular value of the curvature ratio, in both cases the same value of the flutter speed is obtained.

Figure 6 highlights the effects of the mass ratio $\bar{\rho}$. It is clear that for larger values of the mass ratio $\bar{\rho}$ an increase of the flutter speed is experienced. In spite of this, the minimum flutter speed is not affected by the variation of $\bar{\rho}$. Both these results can be shown analytically by using Eq. (41).

Figure 7 shows the implications of the thickness ratio h/b on the flutter Mach number, considered in conjunction with that of the curvature ratio. The results reveal that at relatively small values of the curvature ratio the panels characterized by larger thickness ratios exhibit larger flutter speeds. With the increase of the curvature ratio, the flutter speed decreases and reaches a minimum that strongly depends on the particular value of the thickness ratio. The value of h/R where the minima occur depends on the panel thickness ratio, and with the increase of h/b, these minima shift toward larger values of h/R. Beyond these minima, with the further increase of the curvature ratio, the flutter speed increases.

In Figs. 8 and 9, the effects of the geometric imperfection on the flutter boundary are highlighted, in conjunction with those of curvature and thickness ratios. The results reveal that the imperfections represented in terms of $\hat{q}_1$ and $\hat{q}_2$ reduce the value of the flutter speed. The results of the present investigation are in qualitative agreement with the ones obtained by Barr and Stearman,[42] in the context of aeroelasticity of complete geometrically imperfect circular cylindrical shells.

Figures 10–15 show the Lyapunov first quantity. In Figs. 10–15, the effects of the structural and aerodynamic nonlinearities considered in conjunction with the effect of the curvature and thickness ratios are emphasized. To enhance the understanding on the implications of the curvature on the critical flutter boundary and its character, a generic three-dimensional plot is given in Fig. 10. The intersections of the Lyapunov first quantity $L(M_F; h/b; h/R)$ with the plane $L = 0$ separate the parts of the flutter boundary

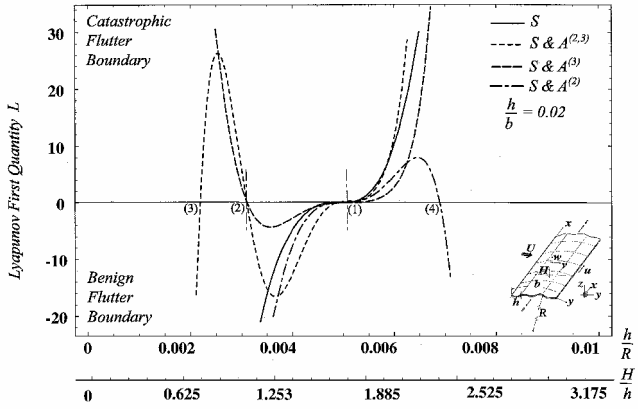

Fig. 11 Benign and catastrophic portions of the flutter boundary vs curvature ratio; effect of structural nonlinearities *S*, aerodynamic quadratic $A^{(2)}$, cubic $A^{(3)}$, and quadratic and cubic $A^{(2,3)}$ nonlinearities, where 1–4 are points of transition from benign to catastrophic flutter boundary and vice versa.

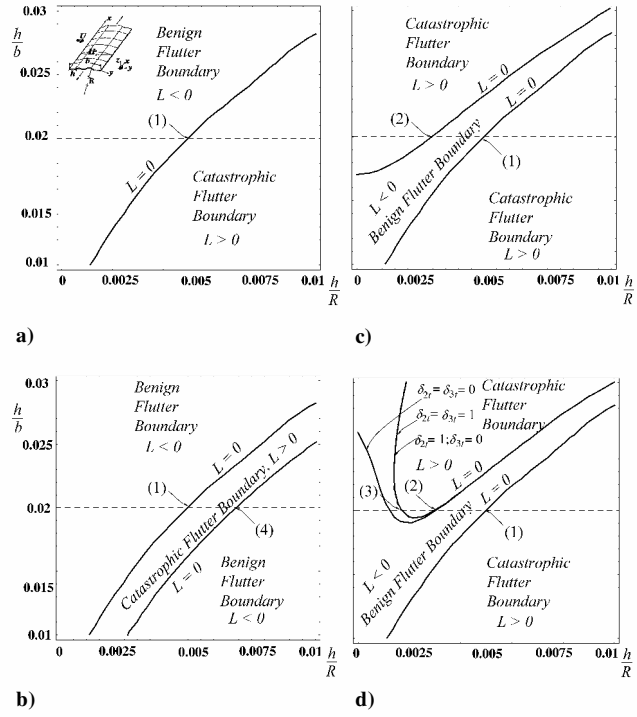

Fig. 12 Benign and catastrophic portions of the flutter boundary as a function of the ratios *h/R* and *h/b*, where 1–4 are the transition points from benign to catastrophic flutter and vice versa and correspond to the cases in Fig. 11. a) Effect of structural nonlinearities only, linear aerodynamics, $\delta_{1y} = \delta_{1t} = 1$ and $\delta_{iy} = \delta_{it} = 0$, $i = 2, 3$, b) Effect of structural and quadratic aerodynamic nonlinearities being retained only, no nonlinear damping, $\delta_{1y} = \delta_{1t} = \delta_{2y} = 1$; $\delta_{2t} = \delta_{3y} = \delta_{3t} = 0$, c) Effect of structural and cubic aerodynamic nonlinearities being retained only, no nonlinear damping, $\delta_{1y} = \delta_{1t} = \delta_{3y} = 1$; and $\delta_{2y} = \delta_{2t} = \delta_{3t} = 0$, and d) Effect of structural nonlinearities and quadratic and cubic aerodynamic nonlinearities, $\delta_{1y} = \delta_{1t} = \delta_{2y} = \delta_{3y} = 1$; effect of the quadratic and cubic damping, $\delta_{2t} = 0; 1$; $\delta_{3t} = 0; 1$.

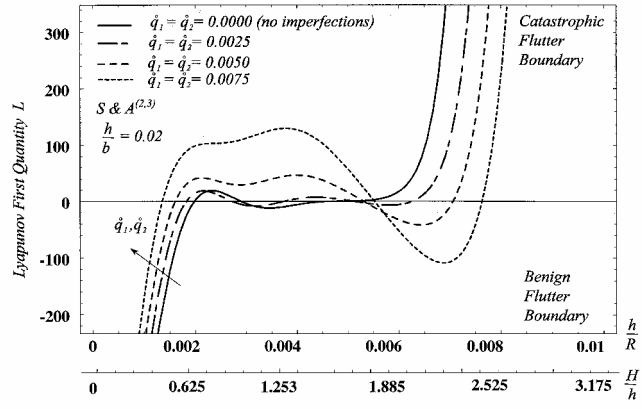

Fig. 13 Benign and catastrophic portions of the flutter boundary in the presence of structural and aerodynamic nonlinearities and imperfections.

that are benign [for $L(M_F; h/b; h/R) < 0$] from the catastrophic ones, for which the opposite relationship is satisfied, namely, $L(M_F; h/b; h/R) > 0$.

Figures 11 and 12 highlight the effect of selected types of nonlinearities considered in conjunction with that of the curvature ratio on the Lyapunov first quantity[39] and implicitly on the character of the flutter boundary. The line $L(M_F) = 0$, identifying the transition between the benign and catastrophic flutter boundary, has been crossed in various points. Point 1 is related to the interaction between the structural nonlinearities and the curvature of the panel, whereas points 2–4 are due to the aerodynamic nonlinearities. In this context, for a certain value of h/R, the slope at which the characteristic curves cross the line $L = 0$ can constitute a measure of the rapidity of transition of the aeroelastic system, from the benign to the catastrophic type of flutter. As can be seen, in the presence of structural nonlinearities S, the transition between the benign and catastrophic flutter boundary occurs at larger values of the curvature ratio, implying that the structural nonlinearities have a stabilizing character, whereas the curvature has a destabilizing influence. Although it was recognized that the aerodynamic nonlinearities A, in general, are destabilizing, it appears that not all of the aerodynamic nonlinearities have this destabilizing characteristics. As was stated in Refs. 4 and 5 and also revealed in the present analysis, under certain conditions aerodynamic nonlinearities can become destabilizing. In addition, as was reported by Karamchati[44] and remarked by Gray and Mei,[37] for flat panels, the term that has the most significant influence on the stable LCO is the quadratic nonlinear aerodynamic one. The present analysis yields the same conclusion and, on the other hand, reveals that the cubic aerodynamic nonlinearities have a destabilizing character in the sense that they have the most significant influence on the unstable LCO. The conclusions related to flat panels can be extracted from Figs. 11 and 12, as a special case of the circular cylindrical panels.

Figure 12a reveals the effects of structural nonlinearities in conjunction with the curvature ratio, on the character of the flutter boundary. In this case, linear aerodynamics is considered. With the increase of the thickness ratio, the transition between benign and catastrophic flutter boundary is shifted toward larger values of the curvature ratio. Quadratic and cubic aerodynamic nonlinearities (with only linear aerodynamic damping) have been considered in Figs. 12b and 12c, respectively. It appears that, although the quadratic nonlinear aerodynamic term is stabilizing in the sense of contributing to the benign character of the flutter boundary (Fig. 12b), the aerodynamic cubic nonlinearities are always strongly destabilizing, contributing to the catastrophic flutter (Fig. 12c).

Because the flow takes place only on one side of the panel, quadratic and cubic nonlinear terms are always present. Some interesting conclusions can be reached from the Lyapunov first quantity. It is clear that the two aerodynamic nonlinearities play different roles on the character of the flutter boundary. In perfect agreement with what was stated in Refs. 14, 35, 37, and 45, the quadratic aerodynamic nonlinear term $(w_{,y})^2$ in the expression of the piston theory has been found to be the most significant one toward determination of the benign character of the flutter boundary. It can be shown from the matrix B_2 (not displayed here) in which the cubic nonlinear aerodynamic term is positive, whereas all of the quadratic nonlinear terms are negative. This implies that the cubic term associated with M_∞^3 has a destabilizing effect on the character of the flutter boundary, whereas an opposite effect is reached by the quadratic term that is associated with M_∞^2. This conclusion can also be reached from Fig. 12b, where the presence of the quadratic aerodynamic nonlinear term extends the benign character of the flutter boundary, as compared to the one from Fig. 12c, in which only the cubic aerodynamic term was included.

Figure 12d shows the effect of nonlinear aerodynamic damping terms $(w_{,\bar{t}})^2$ and $(w_{,\bar{t}})^3$ identified by the tracers δ_{2t} and δ_{3t}. In this

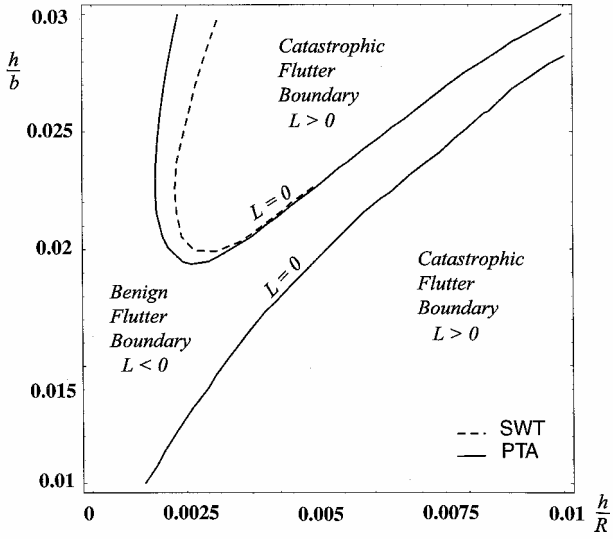

Fig. 14 Benign and catastrophic portions of the flutter boundary for PTA and SWT, as a function of the ratios *h/R* and *h/b*; structural and aerodynamic nonlinearities included.

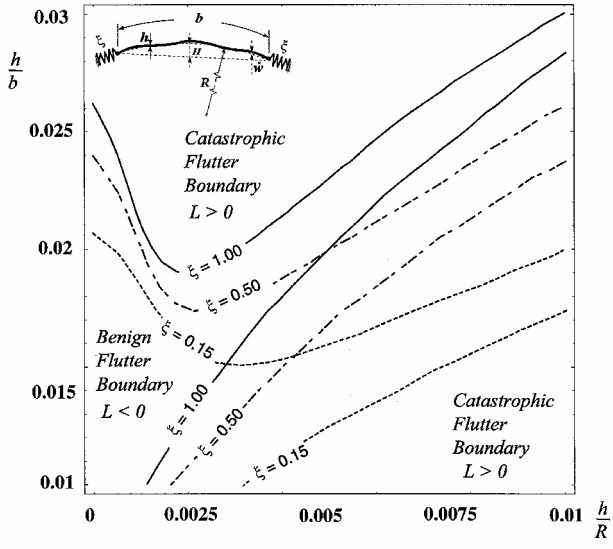

Fig. 15 Benign and catastrophic portions of the flutter boundary for edges partially movable, as a function of the ratios *h/R* and *h/b*; structural and aerodynamic nonlinearities retained and nonlinear damping discarded: ——, Fig. 12c case.

case, quadratic and cubic aerodynamic nonlinear terms $((w_{,\bar{y}})^2$ and $(w_{,\bar{y}})^3)$ are retained in the expression of the unsteady aerodynamics, that is, $\delta_{2y} = 1$ and $\delta_{3y} = 1$. It appears that only the quadratic damping has a significant hardening effect, in the sense of expanding the region belonging to the benign flutter. On the other hand, the nature of the flutter boundary remains unchanged for $\delta_{3t} = 1$ or $\delta_{3t} = 0$. The fact that including or discarding the cubic aerodynamic nonlinear damping $(w_{,\bar{t}})^3$ does not change the nature of the flutter boundary was also reported in Ref. 37.

In Fig. 12, points 1–4, showing the transition between benign and catastrophic flutter boundary regions, correspond to Fig. 11, where $L(M_F) = 0$.

In summary, the following conclusions can be reached from Figs. 11 and 12: 1) The structural nonlinearities *S* provide a stabilizing influence on the panel motion, in the sense that a benign flutter boundary is obtained. 2) The effect of the curvature *C* acts in the opposite sense, and for larger curvatures, a catastrophic flutter boundary is experienced. 3) The aerodynamic nonlinearities *A* have a mixed influence in the sense that they can contribute to produce a supercritical/subcritical Hopf bifurcation, that is, benign/catastrophic flutter boundary, respectively, whenever the quadratic $(A^{(2)})$ or the cubic $(A^{(3)})$ aerodynamic nonlinearities are retained, respectively.

The effect of the imperfections on the Lyapunov first quantity is highlighted in Fig. 13. The presence of imperfections yields a shift of the transition between the stable and unstable states toward lower values of the curvature ratio. This implies that an imperfect cylindrical panel is more prone to a catastrophic flutter than its geometrically perfect counterpart.

The catastrophic and benign portions of the flutter boundary for the cylindrical panel via the use of the PTA and SWT aerodynamic theories are presented in Fig. 14. In addition to what was stated earlier in conjunction with these two theories, from Fig. 14 it is seen that the PTA gives more conservative results (less then 3% difference at the transition flight Mach number). This conclusion clearly appears when comparing the cubic nonlinearities in the two pressure expressions [see Eqs. (20) and (21)], which shows that within the PTA this nonlinear term is larger than that in SWT.

The effects of movable or immovable panel edges are emphasized in Fig. 15, where the effect of the nonlinear aerodynamic damping was discarded, that is, $\delta_{2t} = \delta_{3t} = 0$. In Fig. 15, the parameter identifying the condition of partial movability ξ was chosen to vary from 0.15 (partially movable edges) to 1.00 (immovable edges). For the case of flat panels, with the increases of ξ, a significant increase of the benign portions of the critical flutter boundary is experienced. These predictions are in excellent agreement with Refs. 2 and 4. In addition, from the present analysis, it appears that for circular cylindrical panels the effect of movable or immovable panel edges is more complex, in the sense that, for small curvature ratios, a behavior similar to that of flat panels is experienced, whereas for large curvature ratios, the behavior strongly depends on h/R and h/b ratios.

Conclusions

A number of results and conclusions related to the nature of the flutter instability boundary of infinitely long thin-walled circular cylindrical panels featuring initial geometric imperfections have been presented. In this context, the implications of structural and aerodynamic nonlinearities on the determination of the benign or catastrophic character of the flutter critical boundary have been examined. It was also shown that, at high flight Mach numbers, the cubic aerodynamic nonlinearities contribute invariably toward the catastrophic character of the flutter boundary, whereas the quadratic aerodynamic and structural nonlinearities have an opposite effect, contributing to its benign nature. This implies that, with the increase of the supersonic/hypersonic flight speed, when the cubic aerodynamic nonlinearities become prevalent, the flutter boundary becomes catastrophic, irrespective of the presence of structural and quadratic aerodynamic nonlinearities. In addition, the numerical simulations illustrate that only the quadratic aerodynamic damping has a significant effect and that the nature of the flutter boundary remains unchanged, irrespective of the presence or absence of the cubic aerodynamic damping. As Figs. 5–7 reveal, the curvature ratio plays a complex role in determining the flutter speed whereas, from the point of view of the nature of the flutter boundary in general (see Fig. 14), its influence is detrimental. A comparison of results obtained when PTA and the SWT are used, reveals that the PTA provides more conservative results than those obtained within SWT. Finally, the implications of partially movable and completely immovable panel edges have been highlighted.

Appendix: Expression of Coefficients of Characteristic Equation (35)

$$p = -\left(a_1^{(1)} + a_2^{(2)} + a_3^{(3)} + a_4^{(4)}\right), \qquad p = (2\gamma/\bar{\rho}\overline{\Omega h})\delta_{1t} \tag{A1}$$

$$q = \begin{vmatrix} a_1^{(1)} & a_2^{(1)} \\ a_1^{(2)} & a_2^{(2)} \end{vmatrix} + \begin{vmatrix} a_1^{(1)} & a_3^{(1)} \\ a_1^{(3)} & a_3^{(3)} \end{vmatrix} + \begin{vmatrix} a_1^{(1)} & a_4^{(1)} \\ a_1^{(4)} & a_4^{(4)} \end{vmatrix} + \begin{vmatrix} a_2^{(2)} & a_3^{(2)} \\ a_2^{(3)} & a_3^{(3)} \end{vmatrix} + \begin{vmatrix} a_2^{(2)} & a_4^{(2)} \\ a_2^{(4)} & a_4^{(4)} \end{vmatrix} + \begin{vmatrix} a_3^{(3)} & a_4^{(3)} \\ a_3^{(4)} & a_4^{(4)} \end{vmatrix} \tag{A2}$$

$$q = 17 + \frac{\gamma^2\delta_{1t}}{\bar{\rho}^2\bar{\Omega}^2\bar{h}^2} + \frac{96\hat{h}^2\xi}{\pi^6\bar{h}^4} - \frac{24}{\pi^3\bar{h}^3}\hat{h}\xi\dot{q}_1\dot{\delta}_s \tag{A3}$$

$$r = -\begin{vmatrix} a_1^{(1)} & a_2^{(1)} & a_3^{(1)} \\ a_1^{(2)} & a_2^{(2)} & a_3^{(2)} \\ a_1^{(3)} & a_2^{(3)} & a_3^{(3)} \end{vmatrix} - \begin{vmatrix} a_1^{(1)} & a_2^{(1)} & a_4^{(1)} \\ a_1^{(2)} & a_2^{(2)} & a_4^{(2)} \\ a_1^{(3)} & a_2^{(3)} & a_4^{(3)} \end{vmatrix} - \begin{vmatrix} a_1^{(1)} & a_3^{(1)} & a_4^{(1)} \\ a_1^{(3)} & a_3^{(3)} & a_4^{(3)} \\ a_1^{(4)} & a_3^{(4)} & a_4^{(4)} \end{vmatrix} - \begin{vmatrix} a_2^{(2)} & a_3^{(2)} & a_4^{(2)} \\ a_2^{(3)} & a_3^{(3)} & a_4^{(3)} \\ a_2^{(4)} & a_3^{(4)} & a_4^{(4)} \end{vmatrix} \tag{A4}$$

$$r = \frac{17\gamma\delta_{1t}}{\bar{\rho}\overline{\Omega h}} + \frac{96\hat{h}^2\xi\gamma\delta_{1t}}{\pi^6\bar{\rho}\overline{\Omega h^5}} - \frac{24\hat{h}\dot{q}_1\xi\gamma\delta_{1t}\dot{\delta}_s}{\pi^3\bar{\rho}\overline{\Omega h^4}}, \qquad s = \begin{vmatrix} a_1^{(1)} & a_2^{(1)} & a_3^{(1)}a_4^{(1)} \\ a_1^{(2)} & a_2^{(2)} & a_3^{(2)}a_4^{(2)} \\ a_1^{(3)} & a_2^{(3)} & a_3^{(3)}a_4^{(3)} \\ a_1^{(4)} & a_2^{(4)} & a_3^{(4)}a_4^{(4)} \end{vmatrix} \tag{A5}$$

$$s = 16 + \frac{64M_\infty^2\gamma^2\delta_{1y}}{9\bar{\rho}^2\bar{\Omega}^4\bar{h}^2} + \frac{1536}{\pi^6\bar{h}^4}\hat{h}^2\xi + \frac{256M_\infty\gamma\hat{h}\delta_{1y}\dot{\delta}_s}{\pi^3\bar{\rho}\bar{\Omega}^2\bar{h}^4}\dot{q}_2\xi - \frac{384}{\pi^3\bar{h}^3}\hat{h}\xi\dot{q}_1\dot{\delta}_s \tag{A6}$$

$$a_m^{(j)} = \begin{vmatrix} 0 & 0 & 1 & 0 \\ 0 & 0 & 0 & 1 \\ -1 + \dfrac{24\dot{q}_1\hat{h}\xi\dot{\delta}_s}{\pi^3\bar{h}^3} - \dfrac{96\hat{h}^2\xi}{\pi^6\bar{h}^4} & \dfrac{8M_\infty\gamma\delta_{1y}}{3\bar{\rho}\bar{\Omega}^2\bar{h}} + \dfrac{96\dot{q}_2\hat{h}\xi\dot{\delta}_s}{\pi^3\bar{h}^3} & -\dfrac{\gamma\delta_{1t}}{\bar{\rho}\overline{\Omega h}} & 0 \\ -\dfrac{8M_\infty\gamma\delta_{1y}}{3\bar{\rho}\bar{\Omega}^2\bar{h}} & -16 & 0 & -\dfrac{\gamma\delta_{1t}}{\bar{\rho}\overline{\Omega h}} \end{vmatrix} \tag{A7}$$

$$a_{il}^{(j)} = \begin{bmatrix} [A_1] & [A_2] & [A_3] & [A_4] \\ [A_5] & [A_6] & [A_7] & [A_8] \end{bmatrix}, \qquad j = 3, 4 \tag{A8}$$

$$a_{ilk}^{(j)} = \begin{bmatrix} [B_1] & [B_2] & [B_3] & [B_4] \\ [B_5] & [B_6] & [B_7] & [B_8] \end{bmatrix}, \qquad j = 3, 4 \tag{A9}$$

The elements A_i and B_i ($i = \overline{1, 8}$) of $a_{il}^{(j)}$ and $a_{ilk}^{(j)}$, respectively, are not displayed here, but these can be obtained in a straightforward way from Eq. (34) in conjunction with Eq. (33).

Acknowledgment

The support of this research by the NASA Langley Research Center through Grant NAG-1-01007 is acknowledged.

References

[1]Dowell, E. H., *Aeroelasticity of Plates and Shells*, 1st ed., edited by L. Meirovitch, Mechanics: Dynamical Systems Series, Noordhoff International, Leyden, The Netherlands, 1975, Chap. 3, pp. 35–50, Appendix I, pp. 109–119.

[2]Librescu, L., "Aeroelastic Stability of Orthotropic Heterogeneous Thin Panels in the Vicinity of the Flutter Critical Boundary, Part One: Simply Supported Panels" *Journal de Mécanique*, Pt. 1, Vol. 4, No. 1, 1965, pp. 51–76.

[3]Librescu, L., "Aeroelastic Stability of Orthotropic Heterogeneous Thin Panels in the Vicinity of the Flutter Critical Boundary, Part Two" *Journal de Mécanique*, Pt. 2, Vol. 6, No. 1, 1967, pp. 133–152.

[4]Librescu, L., *Elastostatics and Kinetics of Anisotropic and Heterogeneous Shell-Type Structures, Aeroelastic Stability of Anisotropic Multilayered Thin Panels*, 1st ed., edited by H. Leipholz, Mechanics of Elastic Stability Series, Noordhoff International, Leyden, The Netherlands, 1975, Chap. 1, pp. 53–63, 106–158, Appendix A, pp. 543–552.

[5]Bolotin, V. V., *Nonconservative Problems of the Theory of Elastic Stability*, 1st ed., edited by G. Herrmann, corrected and authorized ed., Macmillan, New York, 1963, Chap. 4, pp. 199–306 (translated from Russian).

[6]Breitbach, E. J., "Effects of Structural Nonlinearities on Aircraft Vibration and Flutter," TR-665, AGARD, Jan. 1978.

[7]Lee, B. H. K., Price, S. J., and Wong, Y. S., "Nonlinear Aeroelastic Analysis of Airfoils: Bifurcation and Chaos," *Progress in Aerospace Sciences*, Vol. 35, No. 3, 1999, pp. 205–334.

[8]Amabili, M., and Pellicano, F., "Nonlinear Supersonic Flutter of Circular Cylindrical Shells," *AIAA Journal*, Vol. 39, No. 4, 2001, pp. 564–573.

[9]Dowell, E. H., "The Flutter of Infinitely Long Plates and Shells, Part 1: Plate," *AIAA Journal*, Vol. 4, No. 8, 1966, pp. 1370–1377.

[10]Dowell, E. H., "The Flutter of Infinitely Long Plates and Shells, Part 2: Cylindrical Shell," *AIAA Journal*, Vol. 4, No. 9, 1966, pp. 1510–1518.

[11]Dowell, E. H., "Nonlinear Flutter of Curved Plates, Part 1," *AIAA Journal*, Vol. 7, No. 3, 1969, pp. 424–431.

[12]Dowell, E. H., "Nonlinear Flutter of Curved Plates, Part 2," *AIAA Journal*, Vol. 8, No. 2, 1970, pp. 259–261.

[13]Dowell, E. H., and Voss, H. M., "Theoretical and Experimental Panel Flutter Studies in the Mach Number Range 1.0 to 5.0," *AIAA Journal*, Vol. 3, No. 12, 1965, pp. 2292–2304.

[14]Mei, C., Abdel-Motagaly, K., and Chen, R., "Review of Nonlinear Panel Flutter at Supersonic and Hypersonic Speed," *CEAS/AIAA/ICASE/NASA Langley International Forum on Aeroelasticity and Structural Dynamics*, NASA CP-1999-209136/PT 1, edited by W. Whitlow Jr. and E. N. Todd, 1999, pp. 171–188.

[15]Bismarck-Nasr, M. N., *Structural Dynamics in Aeronautical Engineering*, 1st ed., edited by J. S. Przemieniechi, AIAA Education Series, AIAA, Reston, VA, 1999, Chap. 9, pp. 229–289.

[16]Bolotin, V. V., Grishko, A. A., Kounadis, A. N., and Gantes, C. J., "Non-Linear Panel Flutter in Remote Post-Critical Domains," *International Journal of Non-Linear Mechanics*, Vol. 33, No. 5, 1998, pp. 753–764.

[17]Dowell, E. H., and Ilgamov, M., *Studies in Nonlinear Aeroelasticity*, 1st ed., Springer-Verlag, New York, 1988, pp. 29–63, 206–277.

[18]Kim, D. H., and Lee, I., "Transonic and Low-Supersonic Aeroelastic Analysis of Two Degree of Freedom Airfoil with Freeplay Non-Linearity," *Journal of Sound and Vibration*, Vol. 234, No. 5, 2000, pp. 859–880.

[19]Mei, C., "A Finite Element Approach of Nonlinear Panel Flutter," *AIAA Journal*, Vol. 15, No. 6, 1977, pp. 1107–1110.

[20]Hopf, E., "Bifurcation of a Periodic Solution from a Stationary Solution of a System of Differential Equations," *Berlin Mathematische Physics Klasse*, Vol. 94, Sächsischen Akademie der Wissenschaften zu Leipzig, Germany, 1942, pp. 3–32.

[21]Sheta, W. F., Harrand, V. J., Thompson, D. E., and Strganac, T. W., "Computational and Experimental Investigation of Limit Cycle Oscillations of Nonlinear Aeroelastic Systems," *Journal of Aircraft*, Vol. 39, No. 1, 2002, pp. 133–141.

[22]Holmes, P. J., "Bifurcations to Divergence and Flutter in Flow-Induced Oscillations: A Finite-Dimensional Analysis," *Journal of Sound and Vibration*, Vol. 53, No. 4, 1977, pp. 471–503.

[23]Lighthill, M. J., "Oscillating Airfoils at High Mach Numbers," *Journal of Aeronautical Science*, Vol. 20, No. 6, 1953, pp. 402–406.

[24]Ashley, H., and Zartarian, G., "Piston Theory—A New Aerodynamic Tool for the Aeroelastician," *Journal of the Aerospace Sciences*, Vol. 23, No. 10, 1956, pp. 1109–1118.

[25]Rodden, W. P., Farkas, E. F., Malcom, H. A., and Kliszewski, A. M., "Aerodynamic Influence Coefficients from Piston Theory: Analytical Development and Computational Procedure," The Aerospace Corp., Rept. TDR-169 (3230-11) TN-2, El Segundo, CA, Aug. 1962.

[26]Liu, D. D., Yao, Z. X., Sarhaddi, D., and Chavez, F. R., "From Piston Theory to a Unified Hypersonic–Supersonic Lifting Surface Method," *Journal of Aircraft*, Vol. 34, No. 3, 1997, pp. 304–312.

[27]Chavez, F. R., and Liu, D. D., "Unsteady Unified Hypersonic/Supersonic Method for Aeroelastic Applications Including Wave/Shock Interaction," *AIAA Journal*, Vol. 33, No. 6, 1995, pp. 1090–1097.

[28]Carafoli, E., and Berbente, C., "Determination of Pressure and Aerodynamic Characteristics of Delta Wings in Supersonic–Moderate Hypersonic Flow," *Revue Roumaine des Sciences Techniques. Serie de Mecanique Appliquee*, Vol. 11, No. 3, 1966, pp. 587–613.

[29]Carafoli, E., Mateescu, D., and Nastase, A., *Wing Theory in Supersonic Flow*, 1st ed., International Series on Monographs in Aeronautics and Astronautics, Division 2: Aerodynamics, edited by R. T. Jones and W. P. Jones, Vol. 7, Pergamon, Oxford, 1969, Chap. 11, pp. 463–524.

[30]Thuruthimattam, B. J., Friedmann, P. P., McNamara, J. J., and Powell, K. G., "Aeroelasticity of a Generic Hypersonic Vehicle," AIAA Paper 2002-1209, April 2002.

[31]Garrick, I. E., and Rubinow, S. I., "Flutter and Oscillating Air-Force Calculations for an Airfoil in a Two-Dimensional Supersonic Flow," NACA TN-1158 and NACA TR-846, Oct. 1946.

[32]In Lee, Lee, D. M., and Oh, I. K., "Supersonic Flutter Analysis of Stiffened Laminated Plates Subject to Thermal Load," *Journal of Sound and Vibration*, Vol. 224, No. 1, 1999, pp. 49–67.

[33]Xue, D. Y., and Mei, C., "Finite Element Nonlinear Panel Flutter with Arbitrary Temperatures in Supersonic Flow," *AIAA Journal*, Vol. 31, No. 1, 1993, pp. 154–162.

[34]Fung, Y. C., "Two-Dimensional Panel Flutter," *Journal of the Aerospace Sciences*, Vol. 25, No. 3, 1958, pp. 147–159.

[35]Eastep, F. E., and McIntosh, S. C., Jr., "Analysis of Nonlinear Panel Flutter and Response Under Random Excitation or Nonlinear Aerodynamic Loading," *AIAA Journal*, Vol. 9, No. 3, 1971, pp. 411–418.

[36]Morino, L., "A Perturbation Method for Treating Nonlinear Panel Flutter Problems," *AIAA Journal*, Vol. 7, No. 3, 1969, pp. 405–411.

[37]Gray, C. E., Jr., and Mei, C., "Large-Amplitude Finite Element Flutter Analysis of Composite Panel in Hypersonic Flow," *AIAA Journal*, Vol. 31, No. 6, 1993, pp. 1090–1099.

[38]Zhou, R. C., Xue, D. Y., and Mei, C., "Finite Element Time Domain Modal Formulation for Nonlinear Flutter of Composite Panels," *AIAA Journal*, Vol. 32, No. 10, 1994, pp. 2044–2052.

[39]Bautin, N. N., *The Behaviour of Dynamical Systems Near the Boundaries of the Domain of Stability*, 2st ed., Nauka, Moscow, 1984, pp. 70–77 (in Russian).

[40]Lyapunov, A. M., *Stability of Motion*, Academic Press, New York, 1966, Chap. 1.

[41]Chandiramani, N. K., Librescu, L., and Plaut, R., "Flutter of Geometrically Imperfect Shear-Deformable Laminated Flat Panels Using Non-Linear Aerodynamics," *Journal of Sound and Vibration*, Vol. 192, No. 1, 1996, pp. 79–100.

[42]Barr, G. W., and Stearman, R. O., "Aeroelastic Stability Characteristics of Cylindrical Shells Considering Imperfections and Edge Constraint," *AIAA Journal*, Vol. 7, No. 5, 1969, pp. 912–919.

[43]Yates, J. E., and Zeydel, E. F. E., "Flutter of Curved Panels," Air Force Office of Scientific Research, TR59-163, Midwest Research Inst., Kansas City, MO, Sept. 1959.

[44]Karamchati, K., "Theoretical Studies of Some Nonlinear Aspects of Hypersonic Panel Flutter," NASA CR-89268, No. 4, Aug. 1967.

[45]McIntosh, S. C., Jr., "Effect of Hypersonic Nonlinear Aerodynamic Loading on Panel Flutter," *AIAA Journal*, Vol. 11, No. 1, 1973, pp. 29–32.

P. Weinacht
Associate Editor